J. Mater. Environ. Sci. 7 (3) (2016) 835-844
ISSN : 2028-2508
CODEN: JMESC

Effect of silicon and phosphorus contents in steel on its corrosion inhibition in 5 M HCl solution in the presence of Cetyltrimethylammonium/KI

Y. El Kacimi[1,*], R. Touir[1,2], M. Galai[1], R. A. Belakhmima[1], A. Zarrouk[3], K. Alaoui[1], M. Ebn Touhami[1]

[1] *Laboratory of Materials Engineering and Environment: Modeling and Application, Faculty of Science, University Ibn Tofail BP. 133-14000, Kenitra, Morocco*

[2] *Centre Régional des métiers de l'éducation et de la formation (CRMEF), Avenue Allal Al Fassi, Madinat Al Irfane, BP 6210 Rabat, Morocco.*

[3] *LCAE-URAC 18, Faculty of Science, First Mohammed University, PO Box 717, 60 000 Oujda, Morocco.*

Received 21 Nov 2015, Revised 05 Jan 2016, Accepted 15 Jan 2016
[*]*Corresponding author: E-mail: elkacimiyounes@yahoo.fr (Y. El Kacimi); Phone: +212 6 63 56 65 45*

Abstract
The effect of silicon and phosphorus content in steel suitable for galvanizing on its corrosion inhibition in 5 M hydrochloric acid solution in absence and presence of 100 ppm of Cetyltrimethylammonium combined with 100 mM of KI (mixture) was studied with conventional corrosion monitoring techniques. This study was carried out by using weight loss, potentiodynamic polarization and electrochemical impedance spectroscopy (EIS) measurements. Potentiodynamic polarization measurements showed that the mixture acted as mixed type inhibitor for the three classes. The experimental results have showed that this organic compound revealed a good corrosion inhibition of steels classes A and B than class C. Thus, the inhibition efficiency was about 97 %, 92 % and 76 % for three classes A, B and C respectively. This founding indicated that the corrosion inhibition depended of the steels composition according to their silicon and phosphorus contents.

Keywords: Corrosion inhibition; Steels grade; Acidic media; Electrochemical measurement.

1. Introduction
The NF A 35-503 standard defines three classes of steels (A, B and C) suitable for Hot-dip galvanizing according to their silicon and phosphorus content. The most critical surface preparation step in the galvanizing process is the pickling to remove iron oxides. In addition, over-pickling of metal leads to a rough, blistered coating. Formation of protective film on the steel surface and characterization of metal surface is the major subject of interest. Mild steel is among the most widely used engineering materials such as metal-processing equipment, marine applications, nuclear and fossil fuel power plants, transportation, chemical processing, pipelines, mining and construction. Hydrochloric and sulphuric acids are the most commonly used acids in pickling bath between 5 and 15 % at temperature up to 80 °C [1]. Iron and its alloys as construction materials in industrial sectors has become a great challenge for corrosion engineers or scientists nowadays [2]. Hot-Dip Galvanizing is one of the most effective ways to protect iron or steel from corrosion. Hot-dip Galvanizing is the immersion of iron or steel articles in molten zinc to apply a protective coating. The galvanizing reaction will only occur on a chemically clean surface. Like most coating processes the secret to achieving a good quality coating lies in the preparation of the surface. It is essential that this is free of grease, dirt and scale before galvanizing. Contamination is removed by a series of processes. One of the most important operations in hot dip galvanizing is the surface preparation of the steel.

The quality of the zinc coating depends on the thoroughness of the metal surface preparation prior to dipping the work into the zinc bath. The metal surface should be entirely free from any oil or grease films and also from

any adhering metal oxides, mill scale and rust. Since the galvanizing process is a metallurgical reaction between clean steel and molten zinc, it is critical to prepare the surface so that iron and zinc can easily interdifuse.

The most critical surface preparation step in the galvanizing process is the pickling is to remove iron oxides. On the other hand, over-pickling of metal which leads to a rough, blistered coating.

Normally, all ferrous metals have a surface oxide or scale as a result of high temperature rolling and annealing and this layer must be removed prior to hot dip galvanizing. Pickling is the chemical removal of these oxides from the surface by immersion in an acid solution. The efficiency of the pickling process is mainly dependent on the nature of the oxide present at the surface of the steel, but, also, on process parameters such as bath composition and time duration are relevant. The oxide scale has to be removed from the steel surface before further processing of the steel strip, for instance cold rolling. Furthermore, the influence of defects and their removal must be considered when manufacturing to specifications that relate to certain surface quality requirements. Removal of oxide is carried out within mechanical methods.

When acid concentration, solution temperatures and line speed are not properly balanced, in fact, sheet defects like under pickling or over pickling may happen and their occurrence does have a very serious effect on cold-reduction performance and surface appearance of the finished product. Pickle baths can contain inhibitors, wetting agents, surfactants, foaming agents, or chelates. [3–8].

Most of the efficient inhibitors are used in industry. These compounds mainly contain oxygen, sulphur, nitrogen atoms and/or multiple bonds in the molecule which are adsorbed on metallic surface [9–16]. Their adsorption behavior on metallic surfaces is affected by their molecular structure, surface state and surface excess metal charge, chemical composition for solution, reaction temperature, immersion time, and electrochemical potential at the metal/solution interface [17].

However, synergistic inhibition is an effective means to improve the inhibitive force of inhibitor, to decrease the amount of usage and to diversify the application of inhibitor in acidic media. Actually, many investigations concerning synergistic inhibition have been carried out [18–20].

The purpose of this paper is to study the effect of silicon and phosphorus contents in steel on its corrosion inhibition in 5 M HCl solution in the presence of Cetyltrimethylammonium with iodide ions (mixture) using electrochemical measurements.

2. Experimental details

2.1. Material preparation

The NF A 35-503 standard defines three classes of steels A, B and C suitable for galvanizing according to their silicon and phosphorus content. The compositions of three steels are presented in Table 1.

Table 1: Silicon and phosphorus contents of three classes of steels suitable for galvanizing according to NF A35-503.

	Composition, %wt.		
Steels grade	Si	P	Si + 2,5 P
Steel / Class A	≤ 0,030	-	≤ 0,090
Steel / Class B	≤ 0,040	-	≤ 0,110
Steel / Class C	0,14 ≤ Si ≤ 0,25	≤ 0,040	≤ 0,325

The chemical composition of the sample steels after analyses and classification according to NF A35-503 (Table 1) is shown in Table 2. The specimen's surface was prepared by polishing with emery paper at different grit sizes (from 180 to 1200), rinsing with distilled water, degreasing in ethanol, and drying at hot air.

Corrosion tests were performed on the three steels which have the following chemical composition (wt.%) balanced with Fe. The steels specimens used have a rectangular form 2,5 cm × 2,0 cm × 0,05 cm. The immersion time for weight loss was 6 h at 293 K. After each immersion, the specimens were cleaned according to ASTM G-81 and reweighed to 10^{-4} g for determining corrosion rate [21]. The aggressive solution of 5 M HCl was prepared by dilution of analytical grade 37 % HCl with distilled water. The molecular formula of cetyltrimethylammonium bromide is shown in Table 3.

Table 2: Chemical composition of the three investigated steels

Steel grade	Composition, wt. %											
	C	Mn	Si	P	S	Al	Ca	Mo	Cu	Ni	Sn	Nb
Steel / Class A	0,051	0,196	0,025	0,012	0,005	0,033	0,002	0,009	0,211	0,087	0,031	0,001
Steel / Class B	0,048	0,174	0,037	0,022	0,004	0,041	0,002	0,010	0,219	0,089	0,031	0,001
Steel / Class C	0,041	0,171	0,150	0,021	0,005	0,043	0,002	0,009	0,181	0,074	0,025	0,001

Table 3: Chemical structure of cetyltrimethylammonium bromide

Abbreviation	*Chemical structure*	*Properties*	
		Chemical formula	*Mas. Wt.*
CTAB	$CH_3(CH_2)_{14}CH_2N^+(CH_3)_3Br^-$	$C_{16}H_{33}N(CH_3)_3 - Br$	364,45

2.2 Weight loss measurement

Weight loss experiments were done according to ASTM methods described previously [20, 21]. Tests were conducted in 5 M HCl for 6 h at 293 K. The average weight loss of three substrate sheets could be obtained. The inhibition efficiency (η_w %) was calculated as follows:

$$\eta_w = \frac{\omega_0 - \omega}{\omega_0} \times 100 \qquad (1)$$

where ω_0 and ω are the corrosion rates of mild steel without and with mixture, respectively.

2.3 Electrochemical measurements

For electrochemical measurements, the electrolysis cell was a borrosilcate glass (Pyrex®) cylinder closed by a cap with five apertures. Three of them were used for the electrode insertions. The working electrode was pressure-fitted into a polytetrafluoroethylene holder (PTFE) exposing only 1 cm^2 of area to the solution. Platinum and saturated calomel were used as counter and reference electrode (SCE), respectively. All potentials were measured against the last electrode.

The working electrode was immersed in test solution during one hour until the steady state corrosion potential (E_{corr}) was reached. The cathodic polarization curve was recorded by polarization from E_{corr} towards more negative direction with a sweep rate of 1 mV/s. After this scan, the same electrode was remained in solution until the obtaining of the steady state corrosion potential (E_{corr} ± 0.002 V), and then the anodic polarization curve was recorded from E_{corr} to positive direction with the same sweep rate. These measurements were carried out using Potentiostat/Galvanostat/Voltalab PGZ 100 monitored by a personal computer. Three experiments were performed in each case and the average corrosion rate was reported.

However, the overall current density, i, is considered as the sum of two contributions, anodic and cathodic current i_a and i_c, respectively. For the potential domain not too far from the open circuit, we can consider that both processes obey the Tafel law **[22]**, so we can draw:

$$i = i_a + i_c = i_{corr}\left\{\exp\left[b_a \times \left(E - E_{corr}\right)\right] - \exp\left[b_c \times \left(E - E_{corr}\right)\right]\right\} \qquad (2)$$

where i_{corr} is the corrosion current density (A cm^{-2}), b_a and b_c are the Tafel constants of anodic and cathodic reactions (V^{-1}), respectively. These constants are linked to the Tafel slopes β (V/dec) in usual logarithmic scale given by equation (3):

$$\beta = \frac{\ln 10}{b} = \frac{2.303}{b} \quad (3)$$

The corrosion parameters were then evaluated by means of nonlinear least square method by applying equation (2) using Origin software. However, for this calculation, the potential range applied was limited to ±0.100V around E_{corr}, else a significant systematic divergence was sometimes observed for both anodic and cathodic branches.

The inhibition efficiency is evaluated from the corrosion current densities values using the relationship (4):

$$\eta_{PP} = \frac{i_{corr}^{0} - i_{corr}}{i_{corr}^{0}} \times 100 \quad (4)$$

where i_{corr}^{0} and i_{corr} are the corrosion current densities values without and with mixture, respectively.

2.4 EIS measurements

The electrochemical impedance spectroscopy measurements were carried out using a transfer function analyzer (VoltaLab PGZ 100), with a small amplitude a.c. signal (10 mV rms), over a frequency domain from 100 KHz to 100 mHz with five points per decade. The EIS diagrams were done in the Nyquist representation. The results were then analyzed in terms of an equivalent electrical circuit using Bouckamp program [23].
The inhibiting efficiency derived from EIS, η_{EIS}, calculated using the following equation (5):

$$\eta_{EIS} = \frac{R_p - R_p^0}{R_p} \times 100 \quad (5)$$

where R^0_p and R_p are the polarization resistance values without and with mixture, respectively
In order to ensure reproducibility, all experiments were repeated three times. The evaluated inaccuracy did not exceed 10 %.

3 Results and discussions

3.1 Weight loss studies

The weight loss measurements were conducted in 5 M HCl at 293 K. The corrosion rate values (ω_{corr}) for three classes of steels are presented in Table 4. It is noted that the corrosion rate values depend of steels composition according to their silicon and phosphorus content. It is seen also that the mixture (100 ppm of CTAB + 100 mM of KI) is good inhibitor for the three classes in 5 M HCl which the class A and B present the best performance compared to steel class C. In addition, according to the composition of each steel, it can be noted that the inhibition efficiency of mixture decreases with increased silicon and phosphorus contents on three classes of steels and follows the order : $\eta_{w\ (Steel\ Class\ A)} > \eta_{w\ (Steel\ Class\ B)} > \eta_{w\ (Steel\ Class\ C)}$.

Table 4: Gravimetric results for three steel classes in 5 M HCl without and with mixture at 293 K

Steels composition				*Inhibitors*	*Weight loss parameter*	
Steels grade	*Si*	*P*	*Si+2,5×P*		ω_{corr} *(mg cm^{-2} h^{-1})*	E_w*(%)*
Steel/Class A	0,025	0,012	0,055	00	39,200	-
				Mixture	1,512	97
Steel/Class B	0,037	0,022	0,092	00	40,010	-
				Mixture	3,0140	92
Steel/Class C	0,150	0,021	0,2025	00	43,251	-
				Mixture	10,010	76

3.2 Potentiodynamic polarization curves

Potentiodynamic polarization curves of the three steels in 5 M HCl without and with mixture at 293 K are given in Figures 1, 2 and 3. Their corresponding parameters such as i_{corr}, E_{corr}, β and α were evaluated from the experimental results using equation (2) and summarized in Table 5. In all cases, the correlation factor R^2 is greater than 0.999 indicating a reliable result. Figure 4 shows, as for an example, the results of regressions calculation for the cathodic and anodic scan for steel class A with and without mixture. It can be seen in this figure a good agreement between the calculated and the experimental polarization data.

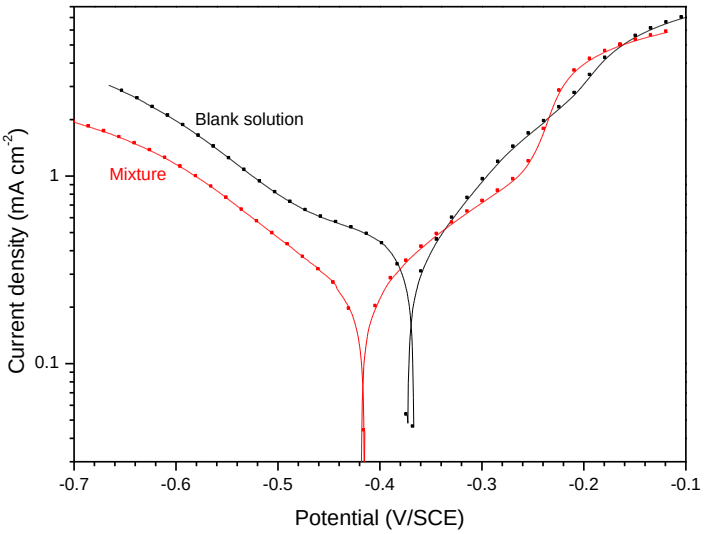

Figure 1: Potentiodynamic polarization curves for steel class A in 5 M HCl in the absence and presence of mixture at 293K.

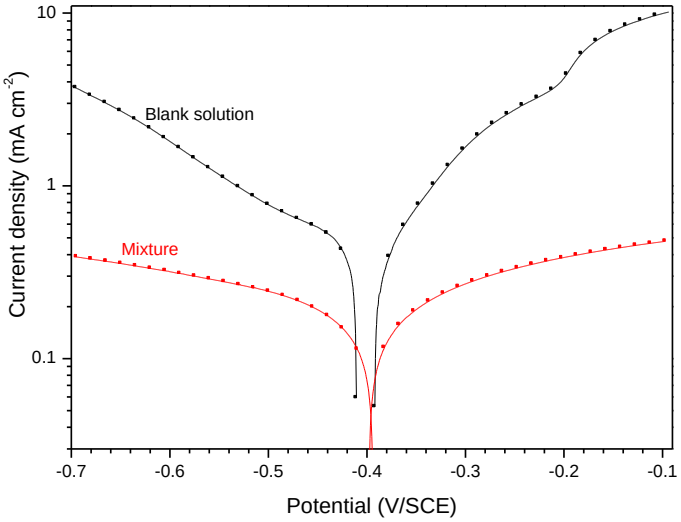

Figure 2: Potentiodynamic polarization curves for steel class B in 5 M HCl in the absence and presence of mixture at 293K.

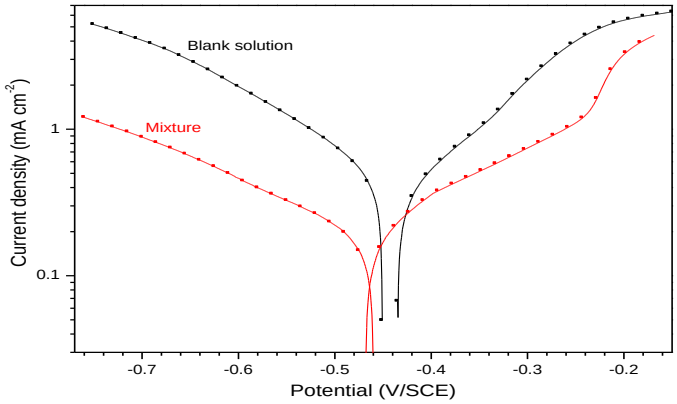

Figure 3: Potentiodynamic i-E curves for steel class C in 5 M HCl in the absence and presence mixture at 293K.

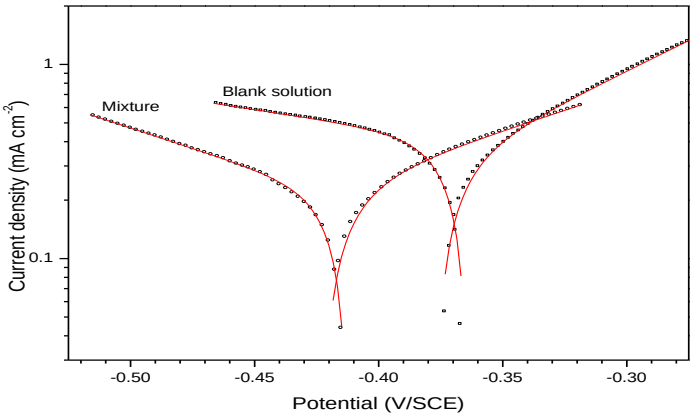

Figure 4: Wide potential range potentiodynamic polarization curves for steel class A in 5 HCl solution in the absence and presence of mixture at 293K. Symbols: Experimental data and Red lines: Fitting data.

However, it can be seen that the mixture addition hinders the acid attack on steel and gives a decrease in anodic and cathodic current densities indicating that the mixture acts as mixed-type inhibitors. Thus, the mixture addition does not change the hydrogen evolution reaction mechanism such as indicated by the slight changes in the cathodic slopes (β) values. This indicates that hydrogen evolution is activation controlled [24, 25]. In addition, it is found that the current densities for steel class A in 5 M HCl without mixture is lesser compared to steel class B and steel class C. This can be attributed to the different of silicon and phosphorus content in their structure.
It has been also observed that inhibition efficiency of mixture for steel class A and steel class B is better than steel class C.
In the other, it is noted that the corrosion rate of the three classes with and without CTAB-KI system increases with increasing the silicon and phosphorus content. The inhibition efficiencies for mixture trail the same evolution vs. the silicon and phosphorus content and follow the order : $\eta_{\text{(Steel Class A)}} > \eta_{\text{(Steel Class B)}} > \eta_{\text{(Steel Class C)}}$.
So, no definite change observed in the corrosion potential (E_{corr}). According to Riggs [26] and others authors, if the displacement in E (i) is > 85 mV/ E_{corr}, the inhibitor can be seen as a cathodic or anodic type, (ii) if displacement in E is < 85 mV/ E_{corr}, the inhibitor can be seen as mixed type. In our study, the maximum displacement is less than 85 mV/ E_{corr}, which indicates that the mixture is a mixed type inhibitor. The results obtained by the potentiodynamic polarization curves confirm those obtained by weight loss measurements.

Table 5: Electrochemical parameters for steels classes in HCl in the absence and presence of mixture at 293K

Steels grade	Inhibitors	E_{corr} *(mV/SCE)*	i_{corr} *($\mu A\ cm^{-2}$)*	α *($mV\ dec^{-1}$)*	β *($mV\ dec^{-1}$)*	η *(%)*
Steel/Class A	00	-369,00	985,70	115,00	- 98,00	-
	Mixture	-416,00	51,00	109,00	- 88,00	95
Steel/Class B	00	-401,09	1083,55	118,50	- 113,40	-
	Mixture	-396,13	98,85	128,00	- 85,00	91
Steel/Class C	00	-441,00	1210,00	144,00	- 95,60	-
	Mixture	-464,30	273,00	132,00	- 91,00	77

3.3 *Electrochemical Impedance Spectroscopy (EIS)*

In order to compare the information about the kinetics of three steel corrosion in the absence and presence of mixture and to ensure complete characterization of the metal/solution interface. EIS measurements were carried out at open circuit potential at 293 K. Figure 5, 6 and 7 show the obtained Nyquist plots for three classes of steels electrode after 1 h of immersion in 5 M HCl solution with and without mixture.

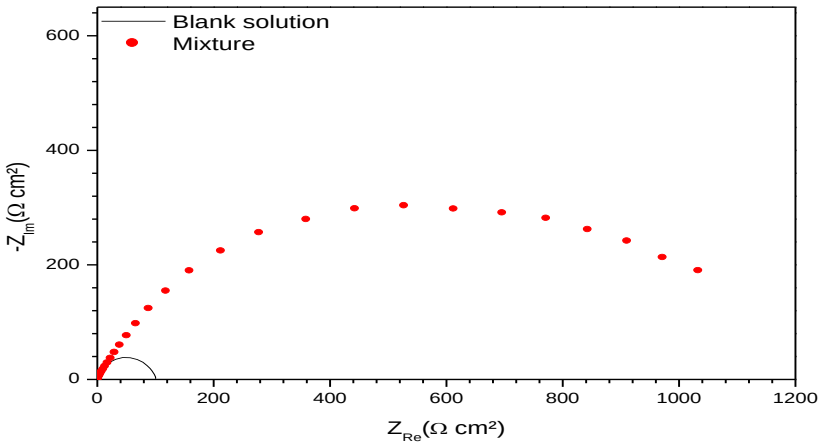

Figure 5: Nyquist diagrams for steel class A in 5 M HCl solution in the absence and presence of mixture at 293K.

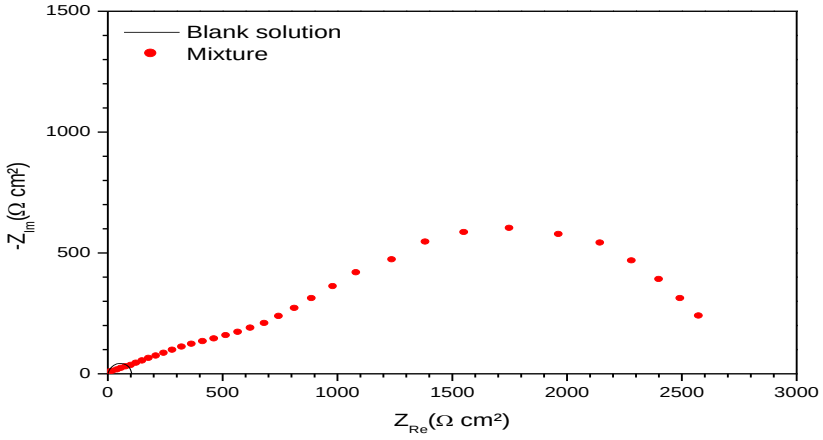

Figure 6: Nyquist diagrams for steel class B in 5 M HCl solution in the absence and presence of mixture at 293K.

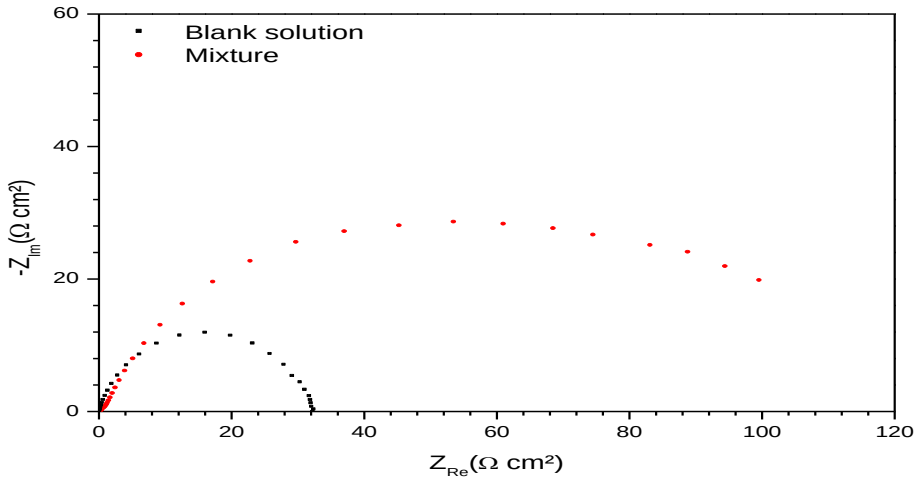

Figure 7: Nyquist diagrams for steel class C in 5 M HCl solution in the absence and presence of mixture at 293K.

It is noted that this plot was composed for one capacitive loop in the absence and presence of mixture for steel classes A and C, indicating that almost no change in the corrosion mechanism with the presence of the inhibitor. This behavior can be attributed to charge transfer of the corrosion process. So, for the steel classe B the plot was composed for two loops in the presence of mixture. It is also noted that the diameter of the semicircle increases with the mixture addition for three classes, indicating an increase in corrosion resistance of the material [27]. It allows employing *CPE* element in order to investigate the inhibitive film properties on metallic surface. Thus, the impedance of the *CPE* can be described by the following equation:

$$Z_{\text{CPE}} = \left[Q(j\omega)^n \right]^{-1} \quad (6)$$

where j is the imaginary number, Q is the frequency independent real constant, $\omega = 2\pi f$ is the angular frequency (rad s^{-1}), f is the frequency of the applied signal, n is the *CPE* exponent for whole number of n = 1, 0, -1, *CPE* is reduced to the classical lump element-capacitor (C), resistance (R) and inductance (L) [28]. The use of these parameters, similar to the constant phase element (*CPE*), allowed the depressed feature of Nyquist plot to be reproduced readily.

However, the effective calculated double layer capacitance (C) derived from the *CPE* parameters according to the following equation [29]:

$$C = Q^{\frac{1}{\alpha}} \times R^{\frac{(1-\alpha)}{\alpha}} \quad (7)$$

The most important data obtained from the equivalent circuit (Figure 8) are presented in Table 6. It may be remarked that R_p value increases and C_{dc} decreases with mixture addition indicating that more inhibitor molecules are adsorbed on metallic surface and provided better surface coverage and/or enhanced the thickness of the protective layer at the metal/solution interface [30, 31]. In addition, these change in R_p and C_{dc} can be attributed to the gradual displacement of water molecules and/or chloride ions on the steel surface [32], leading to a protective solid film, then a decrease in the extent of dissolution reaction [33, 34]. In the other, the decrease of C_{dc} with concentration can be explained by the decrease in local dielectric constant and/or an increase in the protective layer thickness on the electrode surface. This trend is in accordance with Helmhotz model, given by the following equation [35].

$$C_{dc} = \frac{\varepsilon_0 \varepsilon}{e} S \quad (8)$$

where ε is the dielectric constant of the protective layer, ε_0 is the permittivity of free space (8.854 $\times 10^{-14}$ F cm^{-1}) and S is the effective surface area of the electrode.

However, the inhibition efficiencies obtained from electrochemical impedance measurements, increase with mixture addition and show the same trend as those obtained from potentiodynamic polarization and gravimetric measurements. The electrochemical impedance study shows that the use of mixture significantly increases the resistance polarization values and decreases the double layer capacitance in 5 M HCl, suggesting that the corrosion inhibition takes place by simple adsorption. In addition, it is found also that the resistance polarization for steel class A in 5 M HCl without mixture is greater compared to steel class B and steel class C. This can be attributed to the different of silicon and phosphorus content in their structure such as mentioned above. In the other, the same trend of inhibition efficiencies for mixture which follow the order: $\eta_{\text{(Steel Class A)}} > \eta_{\text{(Steel Class B)}} > \eta_{\text{(Steel Class C)}}$.

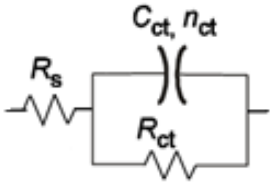

Figure 8: Equivalent circuit model for system Steel / 5 M HCl /mixture.

Table 6: Electrochemical impedance parameters for three steel classes in 5 M HCl solution in the absence and presence of mixture at 293K.

Steels grade	Inhibitors	R_p *(Ω cm²)*	C_{dc} *(μF cm⁻²)*	η_{EIS} *(%)*
Steel/Class A	00	111	269,0	-
	Mixture	2723	22,3	96
Steel/Class B	00	101	282,0	-
	Mixture	1288	39,5	92
Steel/Class C	00	34	312,0	-
	Mixture	144	251,0	76

Conclusion

From the above results and discussions, the following conclusions can be drawn:

- Corrosion rate mild steels in 5 M HCl depends to their compositions in the absence of mixture according on their silicon and phosphorus content, i.e. the corrosion rate increases with increasing of the silicon and phosphorus content.
- A Potentiodynamic polarization measurement indicates that the mixture acts as mixture inhibitors which retarding both the cathodic and anodic process without changing the mechanism of corrosion process for the three classes of mild steels.
- The inhibition efficiency of mixture follows the order: $\eta_{\text{Steel Class A}} > \eta_{\text{Steel Class B}} > \eta_{\text{Steel Class C}}$.
- The electrochemical impedance study shows that the use of mixture significantly increases the polarization resistance values and decreases the double layer capacitance in 5 M HCl, suggesting that the corrosion inhibition takes place by simple adsorption.
- Reasonably good agreement was observed between the obtained data from weight loss measurement, potentiodynamic polarization curves and electrochemical impedance spectroscopy techniques.

References

1. Galai M., El Gouri M., Dagdag O., El Kacimi Y., El Harfi A. and Ebn Touhami M., *J. Chem. Pharm. Res*., 7 (2015) 712.
2. Hazwan Hussin M., Jain Kassim M., Razali N.N., Dahon N.H., Nasshorudin D. *Arab. J. Chem.,* (2011) 1878.
3. Robert M. W., James A. C., The Galvanizing Handbook. Zaclon, Inc., 3 (1996) 271.

4. Colla V., Matarese N., Nastasi G., *International Journal of Soft Computing And Software Engineering*, 1 (2011) 9.
5. Langill T., American Galvanizers Association 303 (1988) 750.
6. Cubberly W. H., Metals Handbook, 9th Edition, Volume 5, Surface Cleaning Finishing, and Coating-American Society for Metals 5 (1990).
7. Tetsuhiko O, Toshinori M, Masaki O, Junya M, European Patent Office (1997).
8. Quraishi M.A., Rawat J., *Materials Chemistry and Physics 73 (2002) 118–122.*
9. El kacimi Y., Achnin M., Aouine Y., Ebn Touhami M., Alami A., Touir R., Sfaira M., Chebabe D., Elachqar A., Hammouti B., *Port. Electrochim. Acta*., 30 (2012) 53.
10. Dehri I., O¨ zcan M., *Mater. Chem. Phys.*, 98 (2006) 316.
11. O¨ zcan M., Dehri I˙., *Prog. Org. Coat*., 51 (2004) 181.
12. Ehteshamzade M., Shahrabi T., Hosseini M.G., *Appl. Surf. Sci.*, 252 (2006) 2949.
13. Lebrini M., Bentiss F., Vezin H., Lagren´ee M., *Corros. Sci.*, 48 (2006) 1279.
14. El-Etre A.Y., Abdallah M., El-Tantawy Z.E., *Corros. Sci.*, 47 (2005) 389.
15. Larabi L., Harek Y., Benali O., Ghalem S., *Prog. Org. Coat.*, 54 (2005) 256.
16. Galal A., Atta N.F., Al-Hassan M.H.S., *Mater. Chem. Phys.*, 89 (2005) 38.
17. Ali J.Z., Guo X.P., Qu J.E., Chen Z.Y., Zheng J.S., *Colloids Surf. A: Physicochem. Eng. Aspects, 281*(2006) 147.
18. Feng Y., Siow K.S., Teo W.K., Hsieh A.K., *Corros. Sci.*, 41 (1999) 829.
19. Zhang D.Q., Gao L.X., Zhou G.D., *J. Appl. Eectrochem*., 33 (2003) 361.
20. Tang L.B., Mu G.N., Liu G.H., *Corros. Sci.*, 45 (2003) 2251.
21. ASTM G-81, Annual Book of ASTM Standards, (1995).
22. Stern M., Geary A.L.. *J. Electrochem. Soc.*, 104 (1957) 56.
23. Boukamp A., Users Manual Equivalent Circuit, ver. 4.51, (1993).
24. Chaudhary R.S., Sharma S., *Indian J. Chem. Technol.*, 6 (1999) 202.
25. Bentiss F., Traisnel M., Lagrene´e M., *Appl. Surf. Sci.*,161 (2000) 196.
26. Riggs JR. O.L., Corrosion Inhibition, second ed., Nathan C.C., Houston TX, (1973).
27. Ghareba S., Omanovic S., *Corro.s Sci.*, 52 (2010) 2104.
28. Gerengi H., Darowicki K., Bereket G., Slepski P., *Corros. Sci.*, 51 (2009) 2573.
29. Brug G.J., Van Den Eeden A.L.G., Sluyters-Rehbach M., Sluyters J.H.. *J. Electroanal. Chem.*, 176 (1984) 275.
30. Moradi M., Duan J., Du X., *Corros. Sci.*, 69 (2013) 338.
31. Tang Y., Zhang F., Huc S., Cao Z., Wu Z., Jing W., *Corros. Sci.*, 74 (2013) 271.
32. Schultze J.W., Wippermann K., *Electrochim. Acta*, 32 (1987) 823.
33. Martinez S, Metikos M., *J. Appl. Electrochem.*, 33 (2003) 137.
34. Hsu C.H., Mansfeld F., *Corrosion*, 57 (2001) 747.
35. Raicheff R., Valcheva K., Lazarova E., Proceeding of the Seventh European Symposium on Corrosion Inhibitors (1990) 48.